Neuroendocrinology Letters Volume 46 No. 8 2025
ISSN: 0172-780X; ISSN-L: 0172-780X; Electronic/Online ISSN: 2354-4716
Web of Knowledge / Web of Science: Neuroendocrinol Lett
Pub Med / Medline: Neuro Endocrinol Lett

ORIGINAL ARTICLE

Modeling Spatial-Temporal Dependencies in Emotion-Related fMRI: A Nonparametric Bayesian Application to the NeuroEmo Dataset

Reza Taherian[1], Seyyed Mohammad Tabatabaei[2], Farzaneh Amanpour[3], Hamid Alavi Majd[4]

1 Department of Biostatistics, School of Allied Medical Sciences, Shahid Beheshti University of Medical Sciences, Tehran, Iran.
2 Department of Medical Informatics, Faculty of Medicine, Mashhad University of Medical Sciences, Mashhad, Iran.
3 Mofid Children's Hospital Clinical Research Development Unit, Shahid Beheshti University of Medical Sciences, Tehran, Iran.
4 Proteomics Research Center, Department of Biostatistics, School of Allied Medical Sciences, Shahid Beheshti University of Medical Sciences, Tehran, Iran.

Correspondence to: Hamid Alavi Majd (Ph.D)
Proteomics Research Center, Department of Biostatistics, School of Allied Medical Sciences, Shahid Beheshti University of Medical Sciences, Tehran, Iran
#41, Darband St., Qods Sq., Tehran, Iran. PostalCode: 1971653313
tel/fax: +98(21)22707347; e-mail: alavimajd@gmail.com

Submitted: 2025-12-17 Accepted: 2025-12-30 Published online: 2025-12-30

Key words: **Functional Magnetic Resonance Imaging; Bayesian Analysis; Brain Mapping; Emotions; India**

Neuroendocrinol Lett 2025; **46**(8):441–448 **PMID:** 41619295 460804 • **www.nel.edu**

Abstract

OBJECTIVES: To characterize the spatiotemporal brain activation patterns evoked by five culturally validated emotion categories—Calm, Afraid, Delighted, Depressed, and Excited—in an Indian sample, and to demonstrate the advantages of a nonparametric Bayesian general linear model (GLM) for naturalistic fMRI data.

MATERIALS & METHODS: Functional MRI data were obtained from 40 healthy, right handed Indian adults (mean age 28.3 ± 9.14 years; 31 males, 9 females) via OpenNeuro (ds005700). Participants viewed 30 s film clips from the Affective Film Dataset from India, interleaved with white noise baselines. Data were preprocessed in SPM12, and regional time series were extracted from 90 cortical/subcortical AAL ROIs using MarsBaR 0.45. We applied the NPBayes fMRI toolbox to fit a spatiotemporal Bayesian GLM with a hierarchical Dirichlet process prior for subject clustering, and spatial basis–function regularization. Posterior inference used Variational Bayes, and activation was declared via posterior probability of inclusion (PPI) thresholded to control a 5% Bayesian false discovery rate.

RESULTS: All emotion conditions engaged early and higher order visual cortices. Calm elicited focal lingual-cuneus activation; Afraid recruited middle/inferior temporal regions; Delighted and Excited amplified visual responses - with Excited also activating parietal attention networks; Depressed combined visual engagement with posterior cingulate/precuneus. The Bayesian framework revealed latent subject subgroups and provided threshold free, reproducible activation maps.

CONCLUSION: Nonparametric Bayesian general linear model analysis of culturally relevant film stimuli yields nuanced insights into emotion-brain dynamics, controls Type I error without arbitrary thresholds, and uncovers interindividual heterogeneity, offering a robust tool for affective neuroimaging.

INTRODUCTION

Functional magnetic resonance imaging (fMRI) is a key tool for investigating the neural basis of emotion, leveraging Blood Oxygenation Level Dependent (BOLD) contrast to measure blood flow and oxygenation changes linked to neural activity. Its high spatial resolution enables identification of brain regions like the amygdala and prefrontal cortex involved in emotional processing, while also capturing temporal dynamics (Lindquist, 2008; Poldrack *et al.* 2011). However, challenges such as inter-subject variability and the multiple comparisons problem complicate the interpretation and generalization of results (Zhang *et al.* 2015).

These issues necessitate advanced statistical modeling, such as random effects analyses and corrections for multiple comparisons, to enhance the reliability and validity of conclusions drawn from fMRI data (Lindquist, 2008; Poldrack *et al.* 2011; Zhang *et al.* 2015). Classical mass-univariate general linear model (GLM) approaches typically analyze each voxel independently and rely on arbitrary spatial smoothing and thresholding procedures, which can obscure subtle spatial dependencies and fail to account for between-subject heterogeneity (Zhang *et al.* 2016).

Understanding when and where the brain responds to emotional stimuli helps reveal how emotions unfold in real time. Spatial patterns show which brain regions are active during different emotions, while temporal patterns capture how fast and how long these responses last. Together, this information improves our understanding of emotion and may help identify brain markers for mood and anxiety disorders. However, most emotional stimulus sets are based on Western samples, which limits their cultural relevance (Lim, 2016; Lindquist *et al.* 2012). To address this, Mishra *et al.* (2023) developed the Affective Film Dataset from India (AFDI), a collection of 69 Indian and Western film clips rated by over 270 Indian participants (Mishra *et al.* 2023). A recent study using the NeuroEmo dataset employed dynamic functional connectivity and graph convolutional neural networks to perform supervised emotion classification (GCNN) (Abgeena *et al.* 2025). In contrast, the present study prioritizes statistical inference and spatiotemporal brain mapping, leveraging nonparametric Bayesian methods to quantify uncertainty and inter-individual heterogeneity rather than prediction.

In this study, we apply a recently proposed nonparametric Bayesian general linear modeling framework for fMRI data, capable of modeling spatial and temporal dependencies, as well as individual heterogeneity within a fully probabilistic framework, to analyze neural responses elicited by the AFDI stimuli (Kook *et al.* 2019; Zhang *et al.* 2016). Our goal is to demonstrate how this method can yield richer, more interpretable insights into the neural correlates of emotion in a culturally relevant setting.

MATERIAL AND METHODS

Dataset

Data for the present study were obtained from the OpenNeuro repository (https://doi.org/10.18112/openneuro.ds005700.v1.2.0), corresponding to the "NeuroEmo: An fMRI Dataset for Emotion Recognition" collection. The dataset comprises functional MRI recordings from 40 healthy, right-handed Indian adults (no history of neurological or psychiatric disorders), who each viewed a series of validated emotional film clips drawn from the AFDI. Participant demographic details (age range, sex distribution) and inclusion/exclusion criteria are provided in the ds005700 metadata on OpenNeuro (Abgeena Abgeena, 2024; Mishra *et al.* 2023). This study was approved by the Ethics Committee of Shahid Beheshti University of Medical Sciences (IR.SBMU.RETECH.REC.1403.191).

Stimuli

Videos used in the emotion-elicitation task were drawn from the AFDI and comprised high-quality 30-second clips selected to evoke five distinct emotion classes: Calm, Afraid, Delighted, Depressed, and Excited. To provide a low-level baseline, each emotion clip was followed by a 30-second white-noise segment, yielding a fixed sequence of 20 epochs over a 10-minute run. Stimuli were presented using an MR-compatible projection system (subtending ~ 20° of visual angle) and delivered binaurally via noise-attenuating headphones. No overt behavioral responses were required during scanning; participants were instructed simply to attend to each clip and let their emotions unfold naturally (Mishra *et al.* 2023).

Data Acquisition

All imaging was performed on a Philips Ingenia 3T MRI scanner at the Central Institute of Psychiatry (CIP), Kanke, Ranchi, using a 32-channel head coil. High-resolution anatomical images were acquired with a T1-weighted sequence (matrix = 192×192×256; voxel size = 1×1×1 mm^3; echo time (TE) = 2.943 ms; repetition time (TR) = 6.5 ms; flip angle = 9°). For structural reference and later spatial normalization, Functional data were collected during two tasks: a resting-state scan and an emotion-elicitation task. Resting-state fMRI used. The resting-state data were collected with a gradient-echo EPI sequence (matrix =

96×96×38; voxel size = 2.29×2.29×4 mm³; slice thickness = 4 mm; inter-slice gap = 4 mm; TE = 35.001 ms; TR = 2.027 s; flip angle = 90°; 38 slices). The emotion-elicitation runs used a similar EPI protocol optimized for task-based activation (matrix = 128×128×36; voxel size = 1.8×1.8×4 mm³; slice thickness = 4 mm; inter-slice gap = 4 mm; TE = 35 ms; TR = 3 s; flip angle = 90°; 36 slices). Each functional run lasted around 10 minutes, and the emotion task followed a block design, where participants viewed 30-second blocks of emotional and white-noise video clips in a fixed sequence. Anatomical scans were used for subsequent coregistration and spatial normalization.

Preprocessing

All functional and anatomical MRI data were preprocessed using SPM 25.01.02 running on MATLAB R2024a, with preprocessing scripts adapted to the dataset's BIDS structure. The pipeline followed standard procedures as outlined in the dataset documentation. First, for each participant, functional images were realigned to correct for head motion using a rigid-body transformation. The mean functional image was then coregistered to the corresponding high-resolution anatomical T1-weighted image. Following coregistration, anatomical images were segmented into tissue classes (gray matter, white matter, CSF), and the transformation parameters were used to normalize both anatomical and functional images to the MNI standard space (voxel size resampled to 2 mm isotropic for functional volumes). Finally, normalized functional images were smoothed using an 8 mm full-width at half-maximum (FWHM) Gaussian kernel to improve the signal-to-noise ratio and account for inter-subject anatomical variability.

To simplify network-level analysis, we extracted regional time series from 90 cortical and subcortical ROIs defined by the Automated Anatomical Labeling (AAL) atlas (excluding cerebellar regions), using the MarsBaR toolbox (version 0.45) in SPM12 following preprocessing.

Model specification

In this study, we applied a spatiotemporal linear regression model to analyze task-related brain activity in multi-subject fMRI data (Monti, 2011; Zhang *et al.* 2016). The model is expressed as

$$Y_{iv} = X_{iv}\beta_{iv} + \varepsilon_{iv}, \quad (1)$$

Where y_{iv} is the BOLD time series at vth ROI (or voxel) in the ith subject, X_{iv} is the design matrix, β_{iv} denotes ROI-wise regression coefficients, and ε_{iv} represents error terms. A hierarchical Dirichlet Process (HDP) prior is applied to β_{iv} to cluster subjects with similar brain responses and address heterogeneity; and also, Spatial correlations are modeled using a Markov Random Field (MRF) prior on selection indicators in a spike-and-slab distribution. Temporal correlations in ε_{iv} are captured by a long memory process, transformed via discrete wavelet transforms (DWT) to enhance computational efficiency (Zhang *et al.* 2016).

The model is extended to accommodate multiple stimuli using a canonical hemodynamic response function (HRF), defined as

$$h_{A_{ivj}} = A_{ivj}\frac{t^{\alpha_1-1}\beta_1^{\alpha_1}}{\Gamma(\alpha_1)} - c\frac{t^{\alpha_2-1}\beta_2^{\alpha_2}}{\Gamma(\alpha_2)}. \quad (2)$$

The design matrix X_{iv} is constructed by convolving stimulus patterns with the canonical HRF, resulting in

$$X_{ivj}(t) = \int_0^t x_j(s)h_{A_{ivj}}(t-s)ds, \quad (3)$$

for each condition j. Posterior inference is performed using a variational Bayes (VB) algorithm, approximating the posterior $P(\beta_{iv}|y_{iv},X_{iv})$. This VB approach offers computational efficiency over Markov chain Monte Carlo (MCMC) methods, making it suitable for large-scale fMRI datasets. This extension enhances the model's flexibility for analyzing complex tasks across multiple stimuli and subjects (Zhang *et al.* 2016; Zhang *et al.* 2014).

In our ROI-based analysis, we adopted a predefined Bayesian false discovery rate (FDR) of 5% and used it to determine the posterior probability of inclusion (PPI) threshold for declaring regions "active." Specifically, we computed each AAL-90 region's PPI, sorted these 90 PPIs in descending order, and selected the largest index v such that

$$FDR_{ij}(k_{ij}) = \frac{\sum_{v=1}^{90}(1-PPI_{ivj})I_{(PPI_{ivj}>k_{ij})}}{\sum_{v=1}^{90}I_{(PPI_{iv}>k_i)}}. \quad (4)$$

This procedure yields a PPI cutoff that guarantees the expected proportion of falsely declared active ROIs does not exceed 5%.

The analysis was conducted using the NPBayesfMRI toolbox, which implements the nonparametric Bayesian modeling framework and supports efficient inference and visualization of activation maps (Kook *et al.* 2019;).

RESULTS

Overview of data

The study sample consisted of 40 healthy Indian adults (31 males, 9 females) with a mean age of 28.3 years (± 9.14 years), recruited specifically to span a young-to-middle adulthood demographic. Participants were all of Indian origin, reflecting the target population for the AFDI (Abgeena *et al.* 2025).

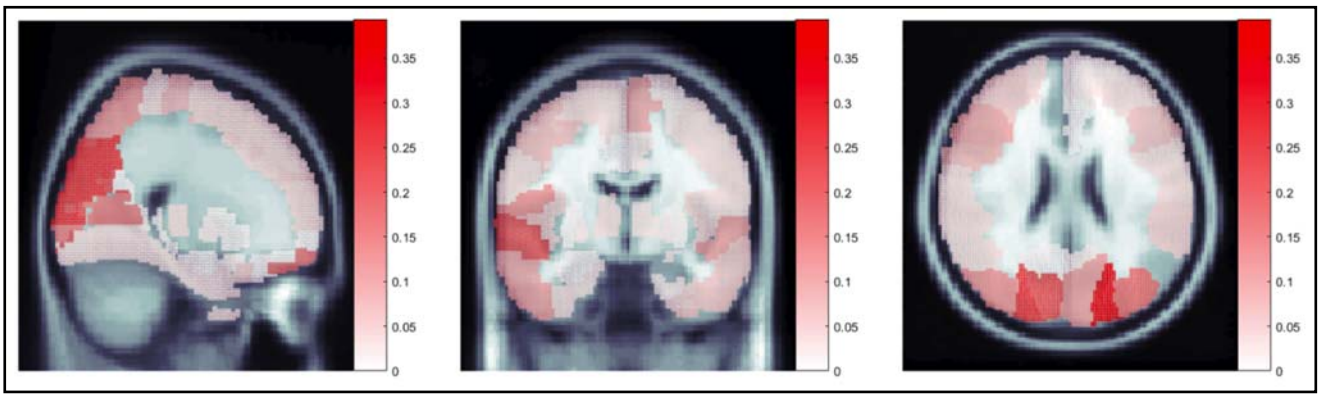

Fig. 1. Calm film viewing predominantly activates early visual cortex in lingual gyrus and cuneus.
ROI-wise posterior mean activation for the Calm condition, shown on sagittal (left), coronal (center), and axial (right) slices at MNI [46, 80, 65].
Note: Low-arousal Calm stimuli elicit focal occipital engagement with minimal limbic activation, reflecting sustained visual attention without emotional salience.

Whole-Brain Activation Maps: Calm Condition

The ROI-wise posterior mean activation map for the Calm condition (Figure 1) was thresholded at a fixed false discovery rate (FDR) of 0.05149, corresponding to a PPI ≥ 0.90437. The most prominent activation cluster was located in the occipital lobe, centered around MNI coordinates [X = 46, Y = 80, Z = 65], corresponding to the lingual gyrus and surrounding visual association cortex. This suggests sustained visual engagement even during low-arousal film clips. Additional posterior effects were observed in the inferior temporal cortex and posterior fusiform gyrus, bilaterally, which are associated with object and scene recognition. These regions consistently exceeded the posterior significance threshold, and the 95% credible intervals for their estimated coefficients excluded zero. In contrast, medial prefrontal and limbic regions were largely inactive under the Calm condition, reflecting the absence of emotional salience or arousal in the presented stimuli.

Whole-Brain Activation Maps: Afraid Condition

The posterior mean activation map for the Afraid stimuli (Figure 2) was thresholded at a fixed FDR of 0.056104, corresponding to a posterior probability of inclusion (PPI) ≥ 0.88437. A strong bilateral activation pattern is evident, with peak activation centered at MNI [X = 52, Y = 81, Z = 56], located in the middle temporal gyrus and extending into the fusiform gyrus and inferior temporal cortex. These regions are consistently implicated in visual threat processing, particularly for dynamic and complex stimuli such as emotional film clips.

Additional clusters are observed in the superior temporal sulcus and posterior insula, reflecting multimodal sensory integration and interoceptive awareness, processes frequently engaged during fearful experiences. While classical limbic structures like the amygdala and anterior cingulate cortex appear less prominent, the widespread posterior cortical engagement suggests heightened visual vigilance and

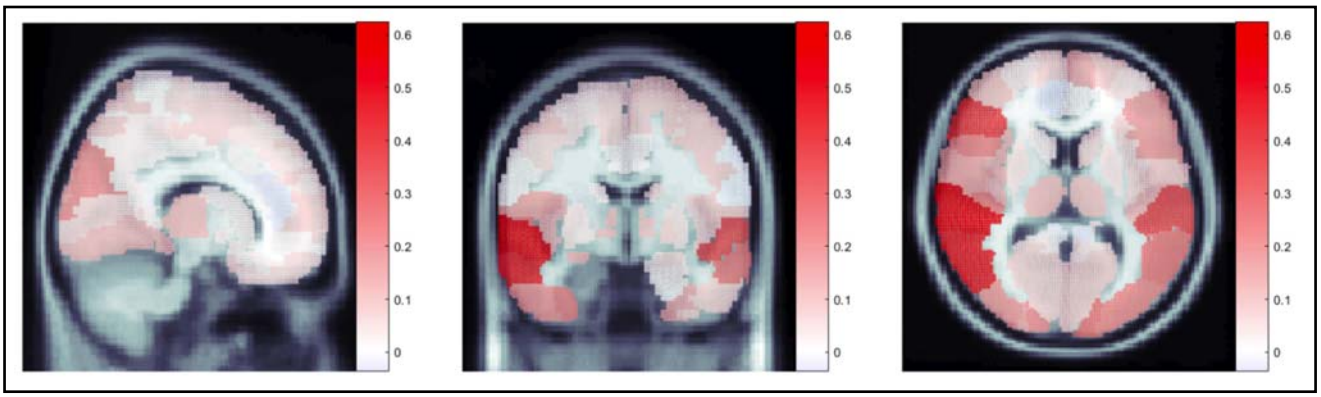

Fig. 2. Threat-related stimuli engage middle and inferior temporal visual processing regions
ROI-wise posterior mean activation for the Afraid condition, shown on sagittal (left), coronal (center), and axial (right) slices at MNI [52, 81, 56].
Note: Fear-evoking stimuli predominantly recruit posterior visual association cortex for dynamic threat evaluation, with limited cortical ROI-level engagement of classical limbic structures.

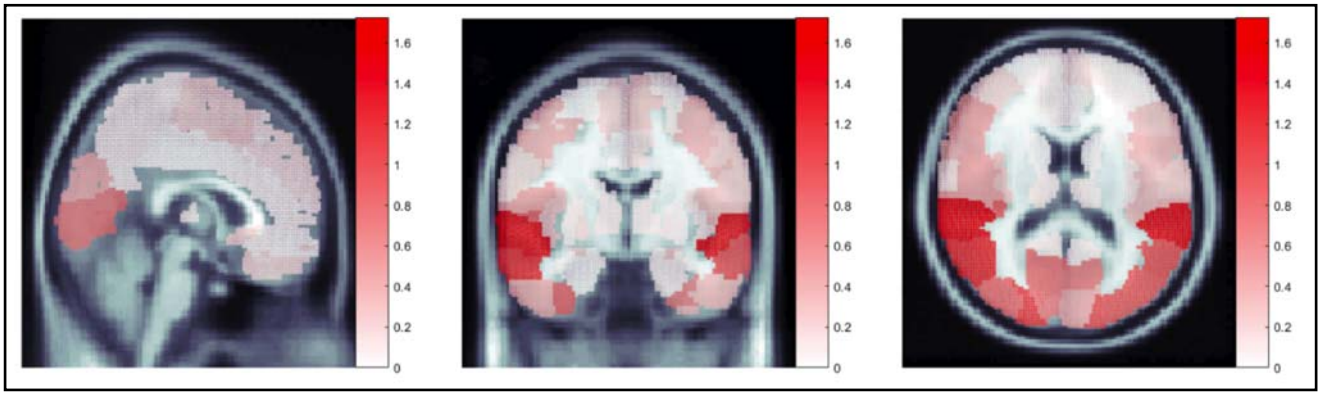

Fig. 3. Positive high-arousal emotions amplify visual cortical responses in lingual and fusiform regions
ROI-wise posterior mean activation for the Delighted condition, shown on sagittal (left), coronal (center), and axial (right) slices at MNI [60, 80, 60].
Note: Delight amplifies perceptual and associative visual networks (posterior mean ~1.6), with minimal medial prefrontal or limbic activation at cortical ROI resolution.

emotional scene processing. The 95% credible intervals of the posterior means in the highlighted regions exclude zero, supporting the robustness of these fear-evoked activations.

Whole-Brain Activation Maps: Delighted Condition

The posterior mean activation map for the Delighted stimuli (Figure 3) was thresholded at an FDR of 0.052185, corresponding to PPI ≥ 0.9032. The peak cluster is centered at MNI [X = 60, Y = 80, Z = 60], located in the right lingual gyrus and adjacent calcarine cortex, indicating robust engagement of early visual areas during positive, high-arousal film segments. A secondary cluster in the right fusiform gyrus suggests enhanced processing of complex visual features, while bilateral activation in the inferior temporal cortex may reflect object- and scene-based appraisal mechanisms. Unlike the Calm condition, medial prefrontal and limbic regions remain minimally active, implying that Delight in this paradigm primarily recruits enhanced perceptual and associative visual networks rather than core affective hubs. All highlighted clusters exceed the posterior inclusion threshold, with 95% credible intervals excluding zero.

Whole-Brain Activation Maps: Depressed Condition

The posterior mean activation map for the Depressed stimuli (Figure 4) was thresholded at an FDR of 0.050649, corresponding to PPI ≥ 0.8532. The principal activation cluster peaks at MNI [X = 60, Y = 80, Z = 70], centered in the right lingual gyrus and extending dorsally into the posterior cingulate cortex/precuneus. This pattern suggests heightened engagement of visual–associative and self-referential networks when viewing negatively valenced, low-arousal film segments. Secondary bilateral clusters emerge in the inferior occipital cortex and posterior fusiform gyrus, indicative of enhanced perceptual processing of emotionally salient scenes. Taken together, these findings point to a combination of visual attention and introspective processing during

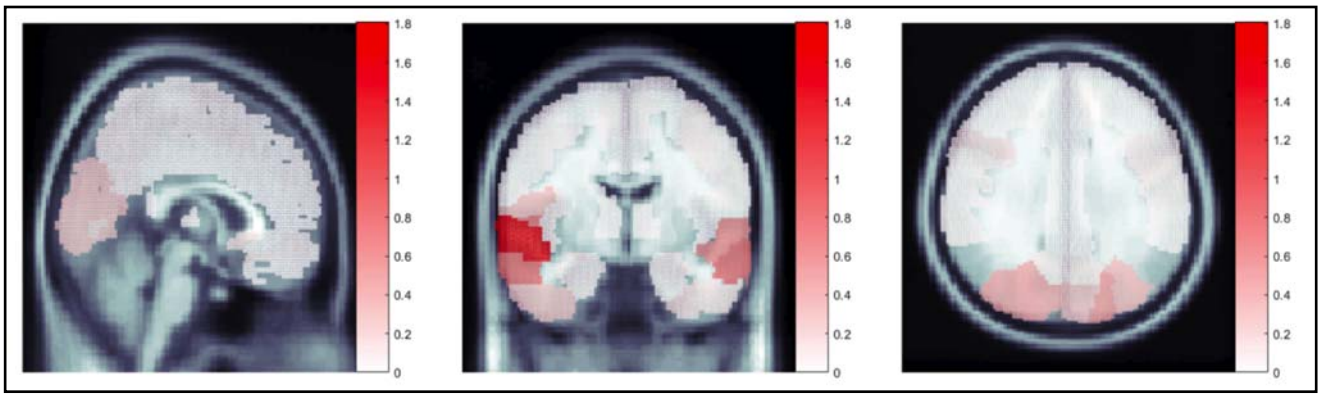

Fig. 4. Depressed mood combines visual processing with default-mode network engagement
ROI-wise posterior mean activation for the Depressed condition, shown on sagittal (left), coronal (center), and axial (right) slices at MNI [60, 80, 70].
Note: Low-arousal negative emotion recruits both visual attention networks and self-referential default-mode hubs, consistent with introspective processing of negatively valenced content.

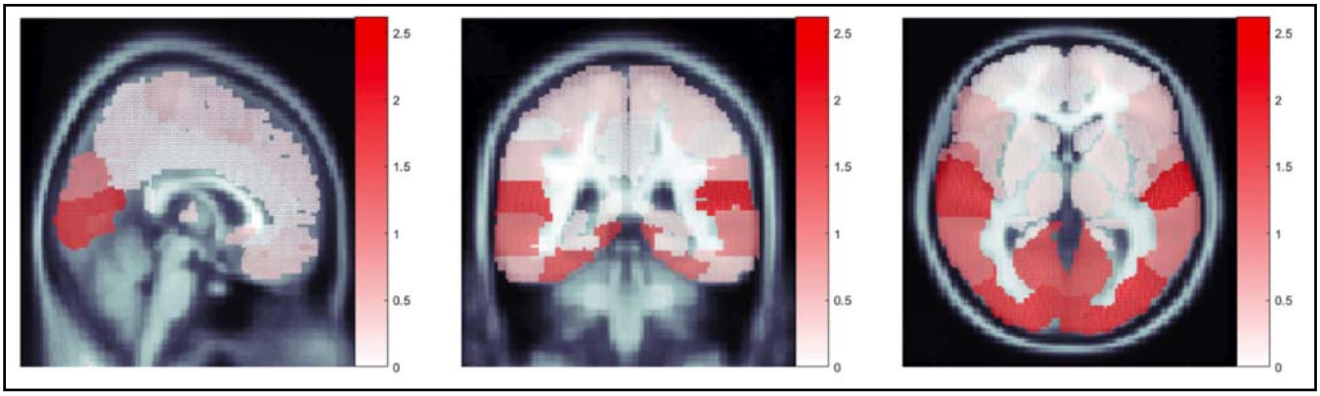

Fig. 5. High-arousal positive emotion (excitement) produces strongest cortical visual activation and parietal engagement
ROI-wise posterior mean activation for the Excited condition, shown on sagittal (left), coronal (center), and axial (right) slices at MNI [60, 60, 50].
Note: High-arousal positive stimuli produce the largest magnitude cortical visual responses among all emotion categories, suggesting valence-dependent amplification of sensory processing.

Depressed stimuli, with all highlighted voxels exceeding the posterior inclusion threshold and their 95% credible intervals excluding zero.

Whole-Brain Activation Maps: Excited Condition

The posterior mean activation map for the Excited stimuli (Figure 5) was thresholded at an FDR of 0.051288, corresponding to PPI ≥ 0.7732. The strongest activation cluster peaks at MNI [X = 60, Y = 60, Z = 50], situated in the right inferior occipital gyrus and extending into the adjacent fusiform gyrus and inferior temporal cortex. This pattern highlights the up-regulation of high-level visual and object-processing areas during high-arousal, positively valenced film segments. Additional bilateral clusters in the middle temporal gyrus and lateral parietal cortex suggest enhanced attentional and multisensory integration processes when participants view exciting content. All suprathreshold voxels exhibit 95% credible intervals that exclude zero, confirming the reliability of these arousal-driven activations.

DISCUSSION

This study aimed to characterize how five culturally validated emotion categories (Calm, Afraid, Delighted, Depressed, Excited) engage distinct brain networks in an Indian sample. We applied a unified nonparametric Bayesian GLM via the NPBayes-fMRI toolbox—using a Dirichlet-process prior for subject clustering and a 5% Bayesian FDR on AAL-90 ROIs—to obtain robust, threshold-free activation maps.

The NPBayes-fMRI model revealed that while the spatial topology of visual cortical engagement was broadly consistent across emotion categories, the magnitude of neural responses varied substantially. However, this pattern does not support a simple arousal-dominance account. Peak posterior means for Excited (~2.5) and Delighted (~1.6) were 4-7 times higher than Calm (~0.35), yet Afraid (~0.3)—despite being classified as a high-arousal negative emotion—showed the weakest activation among all conditions. This dissociation indicates that positive valence, rather than arousal per se, selectively amplifies cortical visual processing during naturalistic film viewing. The potentiated responses observed for positive emotions may reflect enhanced perceptual fluency and approach-motivated attention. In contrast, threat-related stimuli (Afraid) may preferentially engage subcortical vigilance and defensive networks that are not optimally captured by the present AAL-90 cortical ROI analysis. Calm clips produced focal activation in early visual areas (lingual gyrus, cuneus) with minimal limbic involvement. Depressed stimuli combined visual cortex activation with default-mode hubs (posterior cingulate/precuneus), suggesting introspective processing of negative, low-arousal content. Contrary to the classical negativity bias hypothesis, our data did not show stronger responses for threat-related stimuli. Afraid (~0.6) was weaker than both Delighted (~1.6) and Excited (~2.5). Instead, the results suggest that arousal level, regardless of valence, is the dominant factor driving signal amplification. This highlights the importance of considering arousal as the primary modulator of sensory gain in naturalistic emotional contexts.

While the spatial topology of activation was consistent across conditions, the magnitude of the neural response varied by an order of magnitude. Posterior mean activation peaked at ~0.35-0.6 for low-arousal conditions (Calm, Figure 1; Afraid, Figure 2) but surged to ~1.6-2.5 for high-arousal conditions (Delighted, Figure 3; Excited, Figure 5). This large dynamic range in posterior mean activation suggests that emotional context modulates neural gain, selectively amplifying sensory processing under approach-related affective states. The posterior-temporal emphasis in the Afraid condition aligns with models positing that dynamic threat cues are first parsed in high-level visual

regions before engaging limbic circuits (de Gelder & Hadjikhani, 2006; Sabatinelli *et al.* 2007). Our observation that arousal selectively potentiates fusiform and parietal networks supports the view that arousal modulates sensory gain and attentional orienting, whereas valence determines which sensory–associative routes are engaged (Lang & Bradley, 2010). The coupling of visual and default-mode areas in Depressed stimuli highlights how negative valence can trigger self-referential and ruminative processes even in low-arousal contexts (Buckner *et al.* 2008).

Our finding that all five emotion conditions drove strong responses in early and higher-order visual areas highlights the power of dynamic, film-based stimuli to engage perceptual systems. Even in low-arousal states (Calm, Depressed), the lingual gyrus and cuneus were reliably recruited, suggesting that sustained visual attention is a prerequisite for any downstream affective processing. This aligns with work showing that naturalistic scenes evoke more widespread visual activation than static images, effectively "priming" the brain for emotional appraisal (Hasson *et al.* 2010).

By modeling all participants and AAL-90 regions within a single probabilistic framework, we sidestepped the drawbacks of traditional two-stage analyses that first fit each subject separately and then combine results (Friston *et al.* 1995). Spatial basis functions and nonparametric priors provide principled smoothing and yield direct posterior-inclusion probabilities, while variational Bayes makes inference scalable—and the NPBayes-fMRI toolbox ties it all together in a reproducible workflow. (Li *et al.* 2015; Mejia *et al.* 2020).

Despite the strengths of our approach, several limitations warrant consideration. First, our sample comprised 40 healthy, right-handed Indian adults with a mean age of 28.3 years, which may limit the generalizability of findings to other age groups, clinical populations, or cultural contexts. Second, while the nonparametric Bayesian model affords flexible clustering and spatial regularization, it also entails substantial computational demands and relies on variational approximations that can underestimate posterior uncertainty. Third, naturalistic film paradigms, by their very nature, introduce complex, overlapping cognitive and sensory processes that challenge the precise attribution of observed activations to specific emotional dimensions. Finally, the use of an atlas-based cortical ROI framework limits sensitivity to subcortical affective circuitry, which may partially explain the attenuated magnitude observed for threat-related stimuli despite their known high-arousal characteristics.

CONCLUSION

In this study, we applied a nonparametric Bayesian GLM framework to culturally validated film stimuli, uncovering distinct neural signatures of calm, fear, delight, depression, and excitement across visual and introspective networks. Beyond demonstrating methodological advantages, our findings indicate that positive emotional valence selectively amplifies cortical visual processing during naturalistic viewing, whereas high-arousal negative stimuli do not elicit comparable magnitude responses at the cortical ROI level. By leveraging Dirichlet-process clustering and posterior probability thresholding, our approach revealed subtle inter-individual differences and avoided arbitrary statistical cutoffs. These findings not only demonstrate the utility of advanced Bayesian methods for naturalistic fMRI paradigms but also underscore the importance of culturally relevant stimuli in affective neuroscience. Future work should extend this framework to larger, more diverse samples and integrate real-time behavioral measures to further refine our understanding of emotion–brain dynamics.

ACKNOWLEDGMENT

The authors thank "Shahid Beheshti University of Medical Sciences" for research support. We also gratefully acknowledge Keyvan Olazadeh for assistance with ROI time-series extraction.

CONFLICT OF INTEREST

The authors declare no conflicts of interest.

REFERENCES

1 Abgeena A, Garg S, Goyal N, P CJ (2025). NeuroEmo: A neuroimaging-based fMRI dataset to extract temporal affective brain dynamics for Indian movie video clips stimuli using dynamic functional connectivity approach with graph convolution neural network (DFC-GCNN). Comput Biol Med. **194**: 110439. https://doi.org/10.1016/j.compbiomed.2025.110439

2 Abgeena A, Garg S, Goyal N, Raj PC J (2024). NeuroEmo: An fMRI Dataset for Emotion Recognition (Version 1.0.2). https://doi.org/10.18112/openneuro.ds005700.v1.0.2

3 Buckner RL, Andrews-Hanna JR, Schacter DL (2008). The brain's default network: anatomy, function, and relevance to disease. Ann N Y Acad Sci. **1124**: 1–38. https://doi.org/10.1196/annals.1440.011

4 de Gelder B, Hadjikhani N (2006). Non-conscious recognition of emotional body language. Neuroreport. **17**(6): 583–586. https://doi.org/10.1097/00001756-200604240-00006

5 Friston KJ, Holmes AP, Poline JB, Grasby PJ, Williams SC, Frackowiak RS, Turner R (1995). Analysis of fMRI time-series revisited. NeuroImage. **2**(1): 45–53. https://doi.org/10.1006/nimg.1995.1007

6 Hasson U, Malach R, Heeger DJ (2010). Reliability of cortical activity during natural stimulation. Trends Cogn Sci. **14**(1): 40–48. https://doi.org/10.1016/j.tics.2009.10.011

7 Kook JH, Guindani M, Zhang L, Vannucci M (2019). NPBayes-fMRI: Non-parametric Bayesian General Linear Models for Single- and Multi-Subject fMRI Data. Stat Biosci. **11**(1): 3–21. https://doi.org/10.1007/s12561-017-9205-0

8 Lang PJ, Bradley MM (2010). Emotion and the motivational brain. Biol Psychol. **84**(3): 437–450. https://doi.org/10.1016/j.biopsycho.2009.10.007

9 Li F, Zhang T, Wang Q, Gonzalez MZ, Maresh EL, Coan JA (2015). Spatial Bayesian variable selection and grouping for high-dimensional scalar-on-image regression. Ann Appl Stat. **9**(2): 687–713. https://doi.org/10.1214/15-AOAS818

10 Lim N (2016). Cultural differences in emotion: differences in emotional arousal level between the East and the West. Integr Med Res. **5**(2): 105–109. https://doi.org/10.1016/j.imr.2016.03.004
11 Lindquist KA, Wager TD, Kober H, Bliss-Moreau E, Barrett LF (2012). The brain basis of emotion: a meta-analytic review. Behav Brain Sci. **35**(3): 121–143. https://doi.org/10.1017/s0140525x11000446
12 Lindquist MA (2008). The Statistical Analysis of fMRI Data. Stat Sci. **23**(4): 439–464. https://doi.org/10.1214/09-STS282
13 Mejia AF, Yue YR, Bolin D, Lindgren F, Lindquist MA (2020). A Bayesian General Linear Modeling Approach to Cortical Surface fMRI Data Analysis. J Am Stat Assoc. **115**(530): 501–520. https://doi.org/10.1080/01621459.2019.1611582
14 Mishra S, Srinivasan N, Asif M, Tiwary US (2023). Affective film dataset from India (AFDI): creation and validation with an Indian sample. J Cult Cogn Sci. **7**(3): 255–267. https://doi.org/10.1007/s41809-023-00130-6
15 Monti MM (2011). Statistical Analysis of fMRI Time-Series: A Critical Review of the GLM Approach. Front Hum Neurosci. **5**: 28. https://doi.org/10.3389/fnhum.2011.00028
16 Poldrack RA, Mumford JA, Nichols TE (2011). Handbook of Functional MRI Data Analysis. Cambridge University Press. https://doi.org/10.1017/CBO9780511895029
17 Sabatinelli D, Lang PJ, Keil A, Bradley MM (2007). Emotional perception: correlation of functional MRI and event-related potentials. Cereb Cortex. **17**(5): 1085–1091. https://doi.org/10.1093/cercor/bhl017
18 Zhang L, Guindani M, Vannucci M (2015). Bayesian Models for fMRI Data Analysis. Wiley Interdiscip Rev Comput Stat. **7**(1): 21–41. https://doi.org/10.1002/wics.1339
19 Zhang L, Guindani M, Versace F, Engelmann JM, Vannucci M (2016). A spatiotemporal nonparametric Bayesian model of multi-subject fMRI data. Ann Appl Stat. **10**(2): 638–666. https://doi.org/10.1214/16-AOAS926
20 Zhang L, Guindani M, Versace F, Vannucci M (2014). A spatio-temporal nonparametric Bayesian variable selection model of fMRI data for clustering correlated time courses. NeuroImage. **95**: 162–175. https://doi.org/10.1016/j.neuroimage.2014.03.024